AD NUMBER
AD139275
CLASSIFICATION CHANGES
TO: unclassified
FROM: confidential
LIMITATION CHANGES
TO: Approved for public release, distribution unlimited
FROM: Distribution authorized to U.S. Gov't. agencies and their contractors; Administrative/Operational Use; 30 Jun 1969. Other requests shall be referred to Office of Naval Research, Arlington, VA.
AUTHORITY
30 Jun 1969, DoDD 5200.10; ONR ltr, 26 Oct 1977

CONFIDENTIAL

PURDUE UNIVERSITY

AND

PURDUE RESEARCH FOUNDATION

REPORT NO. F-57-1

EXPERIMENTAL ROCKET MOTOR PERFORMANCE AND HEAT TRANSFER OF THE WFNA-AMMONIA AND THE RFNA-AMMONIA PROPELLANT SYSTEMS AT COMBUSTION PRESSURES OF 1000 PSIA AND 1500 PSIA

By

D. G. Elliott

R. K. Rose

Final Report on WFNA-Ammonia and RFNA-Ammonia Investigation

Contract N7 onr 39418

JET PROPULSION CENTER

June 1957

CONFIDENTIAL

ACKNOWLEDGMENTS

The work reported herein was conducted under a research program sponsored by the Office of Naval Research, Contract N7 onr 39418, Task Order 18. The experiments were conducted at the Jet Propulsion Center, Purdue University, under the direction of Dr. M. J. Zucrow, Professor of Gas Turbines and Jet Propulsion.

The authors wish to express their gratitude to Dr. Zucrow for his advice and encouragement during the course of the investigation. They also wish to thank Dr. C. F. Warner and Dr. B. A. Reese for technical advice and for assistance in procuring research equipment and materials.

The authors are indebted to Mr. V. D. Hendricks who operated the instrumentation system, to Mr. L. E. Brenner who fabricated special valves and other items of test equipment, and to Mr. C. D. Merkel and Mr. T. A. Miller who assisted in installing and maintaining the research equipment.

LIST OF FIGURES

LIST OF TABLES

TABLE OF CONTENTS

ABSTRACT

Experimental measurements of the performance and the heat transfer rates of liquid-propellant rocket motors operating at combustion pressures of 1000 psia and 1500 psia have been made with the WFNA-ammonia and the RFNA(15% N_2O_4)-ammonia propellant combinations at mixture ratios (oxidizer/fuel by mass) ranging from 1.0 to 3.4. The rocket motors were convectively water-cooled and had nominal values of thrust = 500 lb, L^* = 100, and contraction ratio = 18; the expansion ratios of the nozzles were such as to give approximately optimum expansion to 14.5 psia atmospheric pressure. The injectors were of the triplet type with six impingement points. The highest values of performance and heat transfer, which were obtained at mixture ratios between 2.0 and 2.3, were as follows (for combustion pressures of 1000 psia and 1500 psia respectively): specific impulse = 237 $lb_f \cdot sec/lb_m$ and 244 $lb_f \cdot sec/lb_m$, specific impulse corrected for heat transfer = 242 $lb_f \cdot sec/lb_m$ and 250 $lb_f \cdot sec/lb_m$, characteristic velocity = 4980 ft/sec and 5040 ft/sec, thrust coefficient = 1.53 and 1.56, average heat transfer rate in the combustion chamber = 2.9 $Btu/in.^2 \cdot sec$ and 3.5 $Btu/in.^2 \cdot sec$, and average heat transfer rate in the nozzle = 7.0 $Btu/in.^2 \cdot sec$ and 9.0 $Btu/in.^2 \cdot sec$. It was found possible to regeneratively cool the rocket motor employed for the experiments at 1000 psia combustion pressure by using the oxidizer (RFNA) to cool the combustion chamber and the fuel (ammonia) to cool the nozzle.

INTRODUCTION

This report presents experimental measurements of performance and heat transfer which were made as part of a continuing program of propellant evaluation which has as its purpose the gathering of performance and heat transfer data, as well as rocket motor design and operating information, at combustion pressures up to 2000 psia using propellant combinations of current interest. The propellant combination used in previous experiments under this program was white fuming nitric acid (WFNA) and jet engine fuel (JP-4). The results of the experiments with WFNA and JP-4, which were conducted at combustion pressures ranging from 300 psia to 2250 psia, were reported in Reference 1.

The experiments reported herein were conducted at nominal combustion pressures of 1000 psia and 1500 psia using the following two propellant combinations: (1) white fuming nitric acid (WFNA) as the oxidizer and anhydrous ammonia as the fuel and (2) red fuming nitric acid (RFNA) containing 15 per cent N_2O_4 as the oxidizer and anhydrous ammonia as the fuel. The latter propellant combination has been investigated previously at combustion pressures ranging from 750 psia to 2160 psia; the previous investigation, which employed rocket motors having approximately 250 lb thrust, was reported in Reference 4.

A different rocket motor was used for each of the two levels of combustion pressure so that the same values of thrust, L^*, and contraction ratio could be maintained. The motors were convectively water-cooled except during two tests at 1000 psia combustion pressure in which regenerative cooling was employed. Firing runs of between one and two minutes duration were made during which the mixture ratio was varied while holding the combustion pressure near the desired value of either 1000 psia or

1500 psia. Measurements were made of specific impulse, characteristic velocity, thrust coefficient, average heat transfer rate in the combustion chamber, and average heat transfer rate in the nozzle, at mixture ratios (oxidizer/fuel by mass) ranging from 1.0 to 3.4.

EXPERIMENTAL APPARATUS, PROCEDURES, AND INSTRUMENTATION

Two rocket motors were employed for the investigation of nitric acid and ammonia. Except for minor modifications the motor with which the experiments at 1000 psia combustion pressure were conducted was similar to that employed for conducting the investigation of WFNA and JP-4 at 1000 psia combustion pressure reported in Reference 2. The rocket motor with which the experiments at 1500 psia combustion pressure were conducted was the one utilized in the investigation of WFNA and JP-4 at 1500 psia combustion pressure reported in Reference 3. The motors had nominal values of thrust = 500 lb, L^* = 100 and contraction ratio (combustion chamber cross-sectional area/nozzle throat area) = 18. The expansion ratios of the nozzles (nozzle exit area/nozzle throat area) were 7.3 for the rocket motor employed for the investigation at 1000 psia combustion pressure and 10.4 for the rocket motor employed for the investigation at 1500 psia combustion pressure; those expansion ratios were slightly lower than the optimum values, but for both nozzles the loss in thrust coefficient due to underexpansion was calculated to be less than 0.1 per cent. The injectors were of the triplet type with six impingement points; at each impingement point two oxidizer streams impinged on one fuel stream. A turbulence ring was located about 0.25 in. beyond the impingement points. The diameters of the injector orifices were the same for both of the rocket motors and the injection pressure drops were approximately 140 psi for both the fuel and the oxidizer at a mixture ratio of 2.2. Each rocket motor employed a helical

cooling passage in the wall of the stainless steel chamber and in the wall of the copper nozzle, and a coolant passage was also provided in the turbulence ring. Water was the coolant in all of the experiments except for one experiment at 1000 psia combustion pressure in which the nozzle was regeneratively cooled by the fuel (ammonia) and one experiment at 1000 psia in which the nozzle was regeneratively cooled by the fuel and the combustion chamber and the turbulence ring were regeneratively cooled by the oxidizer (RFNA). A more detailed description of the two rocket motors, together with a drawing of one of the rocket motors, is presented in Appendix B.

The propellant feed system and the coolant feed system were the same ones employed for the investigation of WFNA and JP-4 at 1500 psia combustion pressure reported in Reference 3 except that different metering orifices were used for measuring the propellant flow rates and a different method for igniting the propellants was utilized. For the acid-ammonia experiments ignition was obtained by placing, prior to each run, about 6 in. of 1/8-in. diameter lithium wire in the ammonia line between the propellant valve and the rocket motor; when the flow of liquid ammonia started the lithium dissolved making the ammonia first entering the combustion chamber hypergolic with the nitric acid. In all of the runs with water-cooling the ammonia was supplied to the rocket motor at the ambient temperature in the test cell (60°F to 80°F).

The ammonia used in the investigation was commercial anhydrous ammonia containing 99.5 per cent NH_3. The white fuming nitric acid (WFNA) was specified when purchased to contain not less than 98.5 per cent HNO_3, and the red fuming nitric acid (RFNA) was specified to be in accordance with government specification MPD-138-A (15% $\pm$ 1% N_2O_4).

3% ± 0.5% H_2O, 80.0% to 83.5% HNO_3, 0.5% ± 0.1% HF, 0.1% maximum solids). No analyses were made to check the composition of the acids, but the specific gravities were found to correspond to the specified percentages of N_2O_4 and H_2O.

The instrumentation was the same as that employed for the tests of WFNA and JP-3 at 1500 psia reported in Reference 3. Flow rates were measured with orifice meters and the thrust, the pressures, and the differential pressures were measured with Wiancko pickups and recorded on Brown "Electronik" strip-chart recorders. The coolant temperatures were measured by iron-constantan thermocouples and were recorded on Brown strip-chart recorders.

During each run the mixture ratio was varied in steps while the combustion pressure was maintained near the desired level of either 1000 psia or 1500 psia. The required variations in the propellant flow rates were obtained by raising the propellant tank pressures and by operating throttle valves in the propellant feed lines; the valves were remotely actuated by an operator who was guided in making the adjustments by meters indicating the propellant flow rates and the combustion pressure. After establishing each mixture ratio the rocket motor was permitted to run for 16 to 20 seconds with no further adjustments of either the tank pressures or the throttle valves thus giving steady-state operation. Ordinarily, it was possible to hold the combustion pressure to within 30 psi of the desired value, but greater deviations sometimes occurred because of limitations in the control apparatus; some of the measurements reported herein were therefore obtained at combustion pressures differing by as much as 90 psi from the nominal values of either 1000 psia or 1500 psia.

EXPERIMENTAL PERFORMANCE

The performance and heat transfer data obtained from all of the experiments in which valid measurements were made are tabulated in Appendix E. Each value tabulated is the average value measured during at least five seconds of steady operation. Values of the estimated errors in the measured values of performance and heat transfer are presented in Appendix F.

The measured values of specific impulse I_s, specific impulse corrected for heat transfer I_{s_a}, characteristic velocity c^*, and thrust coefficient C_F, are plotted as a function of mixture ratio (mass flow rate of oxidizer/mass flow rate of fuel) in Figures 1 through 7. The values of specific impulse corrected for heat transfer, I_{s_a}, were obtained by adding to the measured specific impulse, I_s, the additional specific impulse which it was calculated would be obtained if there were no heat transfer to the rocket motor walls. The added specific impulse was a maximum of 6.5 $lb_f \cdot sec/lb_m$ for the maximum heat transfer rates which were obtained in the tests. The definitions and formulas used in computing I_s, c^*, C_F, and I_{s_a} are presented in Appendix C.

Also plotted in Figures 1 through 7 are curves which show the percentages of the theoretical (frozen composition) performance values which were found to best fit the experimental data over the mixture ratio range from 1.0 to 3.4. The theoretical performance values from which these curves were obtained were extrapolated from the theoretical (frozen composition) performance values presented in Reference 5 for combustion pressures up to 800 psia; the method of extrapolation in described in Appendix D.

As can be seen from Figures 1 through 7 the performance obtained with RFNA as the oxidizer was substantially the same as the performance obtained with WFNA as the oxidizer. The highest values of I_s and c^* were

obtained at mixture ratios between 2.0 and 2.3. The measured values of I_s, I_{s_A}, c^* and C_F at a mixture ratio of 2.0, as given by the fitted curves, together with the corresponding percentages of the theoretical performance were as follows:

TABLE I

Measured Performance Values at r = 2.0 and the Corresponding Percentages of the Theoretical (Frozen Composition) Performance Values

Performance Parameter	Performance at 1000 psia Combustion Pressure	Performance at 1500 psia Combustion Pressure
I_s	237 $lb_f \cdot sec/lb_m$	244 $lb_f \cdot sec/lb_m$
	91 per cent	91 per cent
I_{s_A}	242 $lb_f \cdot sec/lb_m$	250 $lb_f \cdot sec/lb_m$
	93 per cent	93 per cent
c^*	4980 ft/sec	5040 ft/sec
	94 per cent	95 per cent
C_F	1.53	1.56
	97 per cent	96 per cent

The values of I_s, c^*, and C_F for the two 1000 psia tests with regenerative cooling (one test having regenerative cooling of the nozzle only) are shown together with the values of I_s, I_{s_A}, c^*, and C_F for the 1000 psia tests with water cooling in Figures 1, 3, 5, and 7. As shown in Appendix C an increase in the value of I_s over the value with water cooling approximately equal to I_{s_A} minus I_s (about 5 $lb_f \cdot sec/lb_m$ for the 1000 psia runs) would be expected for experiments with regenerative cooling of both the combustion chamber and the nozzle. An increase in I_s of about 3 $lb_f \cdot sec/lb_m$ would be

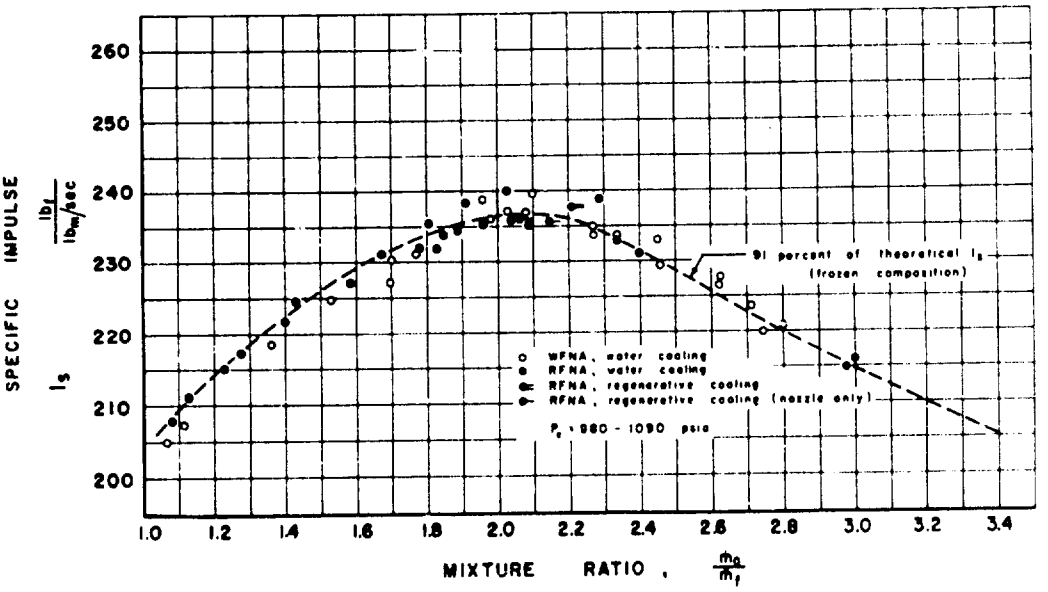

Figure 1. Measured Specific Impulse at 1000 psia Combustion Pressure Compared with Theoretical

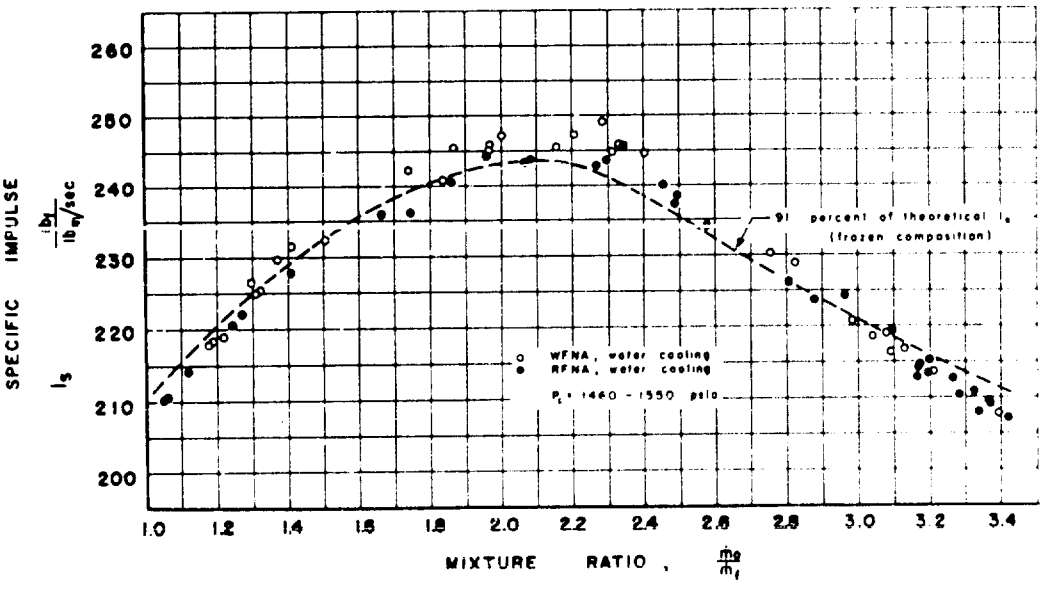

Figure 2. Measured Specific Impulse at 1500 psia Combustion Pressure Compared with Theoretical

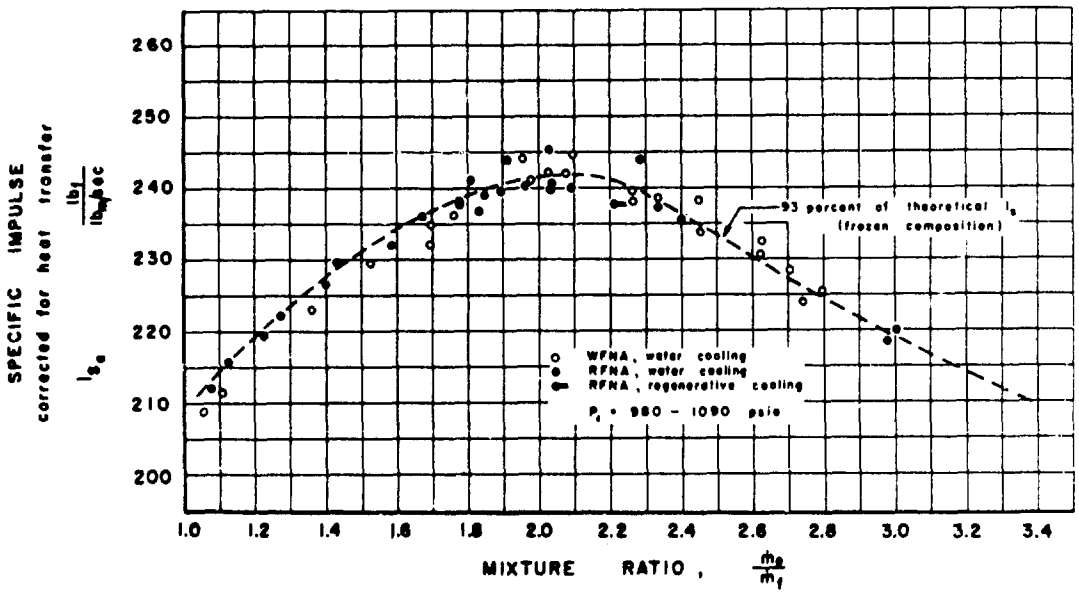

Figure 3. Measured Specific Impulse, Corrected for Heat Transfer, at 1000 psia Combustion Pressure Compared with Theoretical

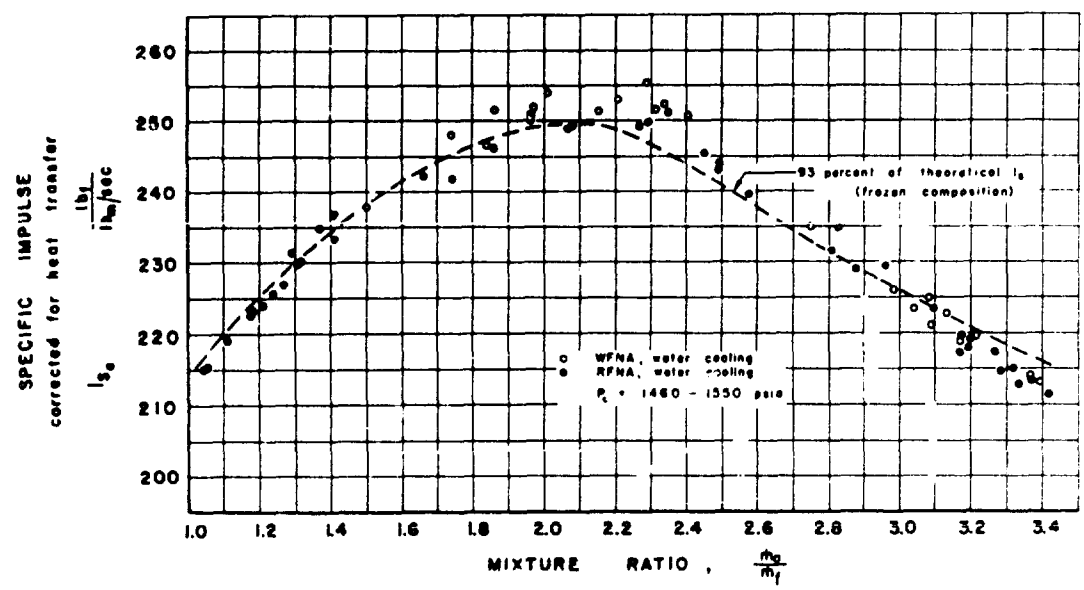

Figure 4. Measured Specific Impulse, Corrected for Heat Transfer, at 1500 psia Combustion Pressure Compared with Theoretical

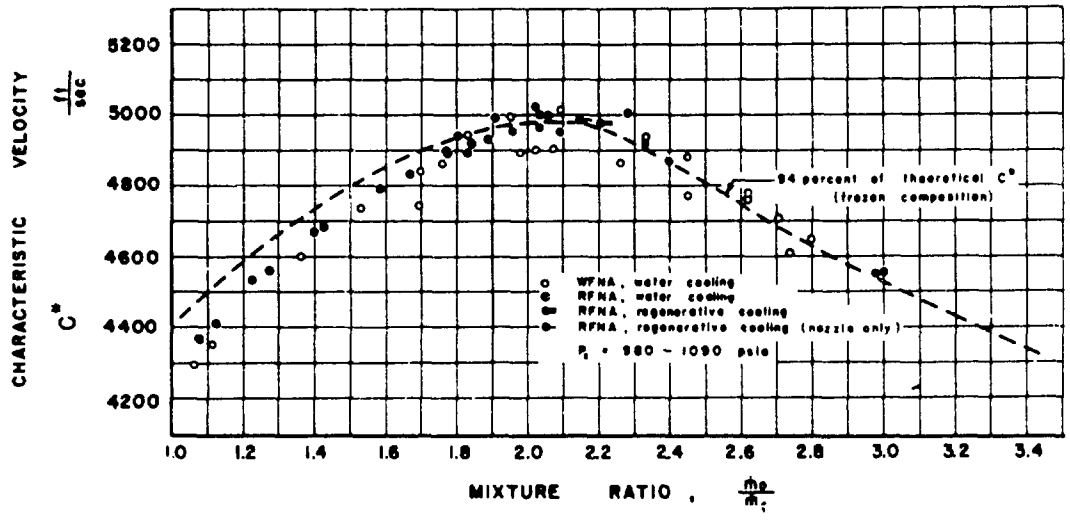

Figure 5. Measured Characteristic Velocity at 1000 psia Combustion Pressure Compared with Theoretical

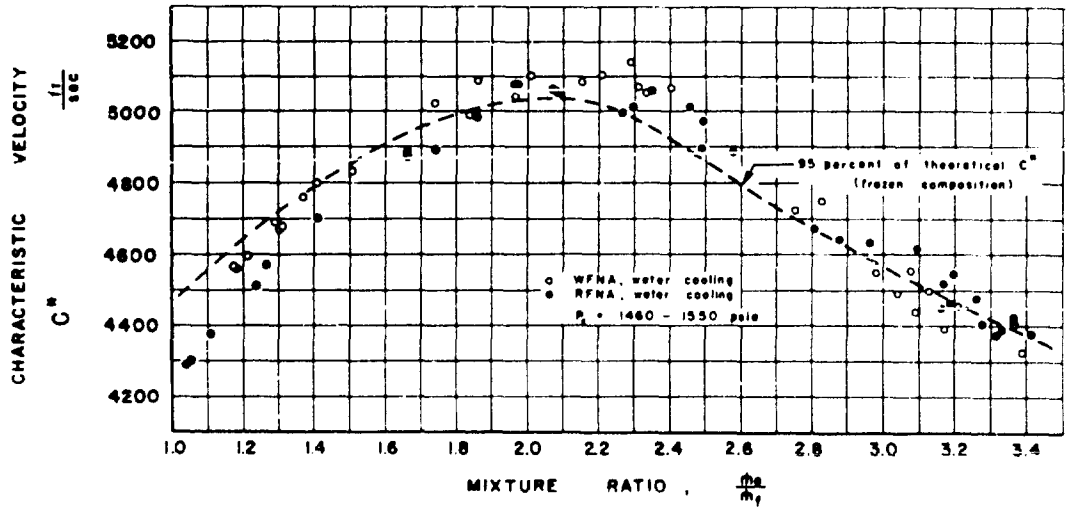

Figure 6. Measured Characteristic Velocity at 1500 psia Combustion Pressure Compared with Theoretical

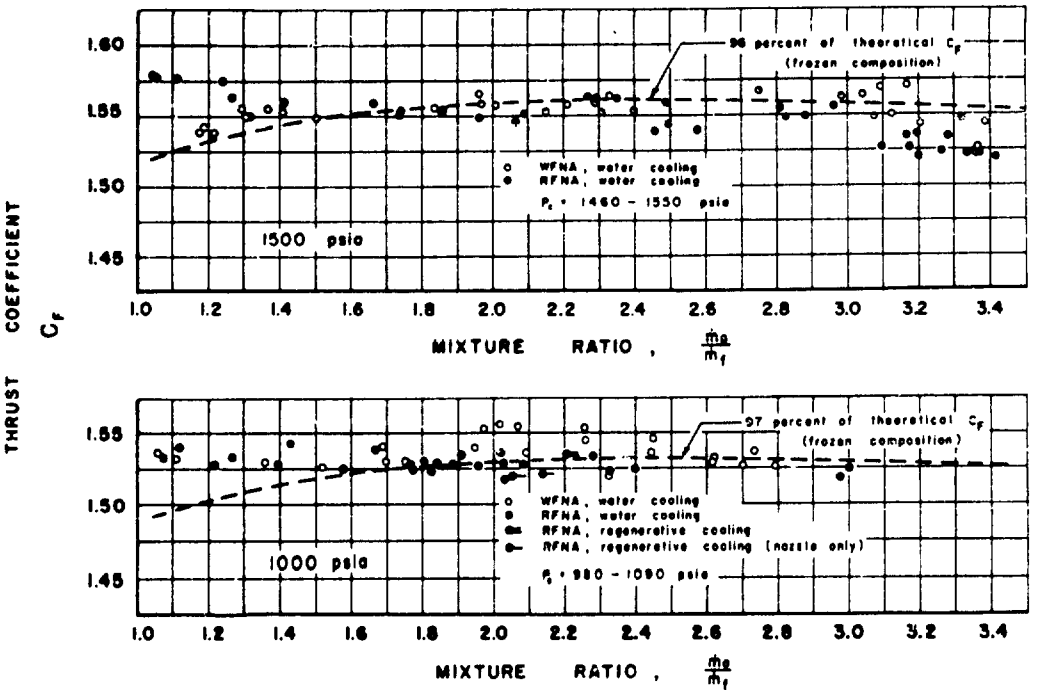

Figure 7. Measured Thrust Coefficient at 1000 psia and 1500 psia Combustion Pressures Compared with Theoretical

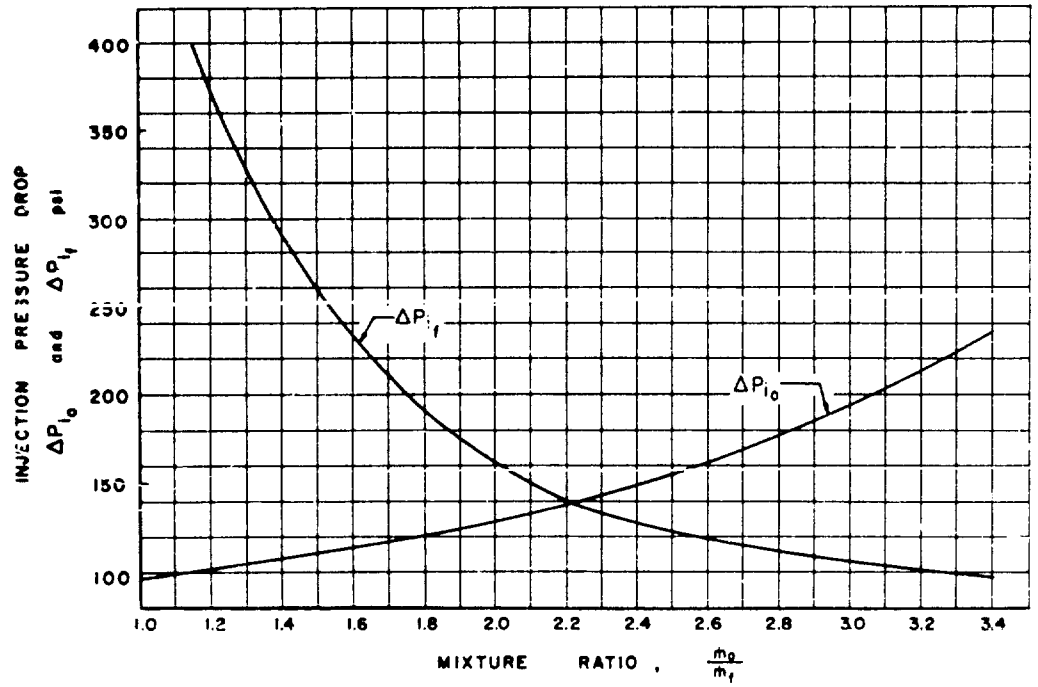

Figure 8. Approximate Pressure Drops in the Injection Orifices of the Research Rocket Motors

expected for experiments with regenerative cooling of the nozzle only. However, these increases in I_s are not clearly shown by the data since the expected increases are of the same magnitude as the scatter in the measured values of I_s. The main result obtained from the experiments with regenerative cooling was that regenerative cooling with acid and ammonia was found to be possible at the high heat transfer rates obtained at 1000 psia combustion pressure. However, very favorable coolant velocities and temperatures, as well as impractically large coolant pressure drops, were utilized in the experiments with regenerative cooling. The ammonia velocity in the coolant passage of the nozzle ranged from 140 ft/sec at the entrance and exit of the nozzle to 240 ft/sec at the throat of the nozzle, and the pressure drop in the coolant passage of the nozzle was 800 psi (inlet pressure = 2000 psia, outlet pressure = 1200 psia). The ammonia was cooled to 30°F or lower before each regeneratively-cooled test. The acid velocity in the coolant passage of the chamber was 50 ft/sec and the pressure drop in that coolant passage was 400 psi (inlet pressure = 1750 psia, outlet pressure = 1350 psia). The acid inlet temperature was 79°F.

The performance obtained with nitric acid and ammonia was lower than the performance which was obtained previously with WFNA and JP-4 employing the same rocket motors. The maximum specific impulse was about 4 per cent lower for the acid-ammonia experiments than for the acid - JP-4 experiments. The maximum c^* and the maximum C_F were about 2 per cent lower for the acid-ammonia experiments than for the acid - JP-4 experiments. The lower values of I_s and c^* obtained with the acid-ammonia propellant combination probably indicate that there was less complete combustion of the acid and ammonia than of the acid and JP-4 since the theoretical performance of the acid-ammonia combination is one to two per cent higher than the theo-

retical performance of the acid - JP-4 combination (as approximated by acid-octane; Cf. Reference 3).

Figure 8 shows the injection pressure drops as a function of mixture ratio for the rocket motor employed for the investigation at 1000 psia combustion pressure; Figure 8 is based on the flow rates corresponding to the fitted theoretical performance curves. The injection pressure drops were approximately 140 psi for both the fuel and the oxidizer at a mixture ratio of 2.2. The injection pressure drops for the rocket motor employed for the investigation at 1500 psia combustion pressure were about 10 per cent lower than the pressure drops shown in Figure 8. The injection pressure drops for the regeneratively-cooled experiments, for which the nozzle throat was enlarged (Cf. Appendix B), were about 200 psi for both the fuel and the oxidizer at a mixture ratio of 2.2.

EXPERIMENTAL HEAT TRANSFER

The values of the average heat transfer rate in the nozzle (heat transferred per second to the coolant divided by the gas-side surface area of the nozzle) and the average heat transfer rate in the combustion chamber (heat transferred per second to the coolant divided by the gas-side surface area of the combustion chamber) are plotted as a function of mixture ratio in Figures 9 and 10. The curves drawn in Figures 9 and 10 show the upper and lower limits which include most of the heat transfer values obtained in the experiments. The large scatter in the values of heat transfer can be only partly attributed to experimental error (Cf. Appendix F); most of the scatter represents actual variations in the heat transfer rates within runs and from run to run, and it is believed that these variations were caused chiefly by the erratic deposition of solid material on the motor walls. After the first test with each rocket motor a dark brown deposit appeared on the

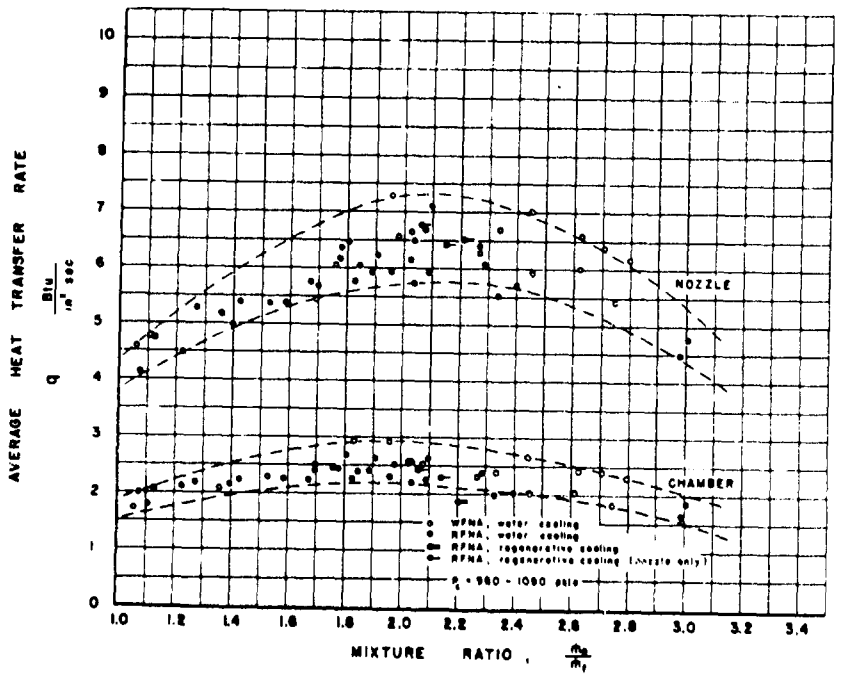

Figure 9. Measured Average Heat Transfer Rate in the Combustion Chamber and in the Nozzle at 1000 psia Combustion Pressure

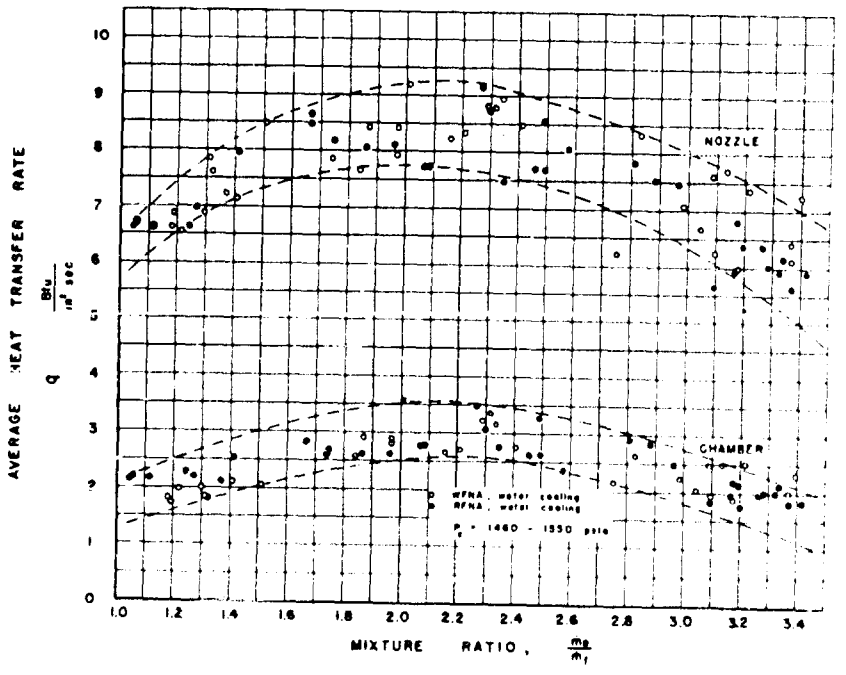

Figure 10. Measured Average Heat Transfer Rate in the Combustion Chamber and in the Nozzle at 1500 psia Combustion Pressure

combustion chamber and nozzle walls which varied from a powdery deposit in the combustion chamber to a hard scale in the convergent section and throat of the nozzle. The extent and thickness of the deposit appeared to change somewhat from run to run, and the deposit was not removed between runs. Since samples of the deposit were strongly attracted by a magnet it is believed that the deposit was chiefly iron oxide from the nitric acid.

As can be seen from Figures 9 and 10 the heat transfer rates obtained with RFNA as the oxidizer were substantially the same as the heat transfer rates obtained with WFNA as the oxidizer. The maximum heat transfer rates, which occurred at a mixture ratio of approximately 2.0, were about 2.9 Btu/in.^{2}·sec in the combustion chamber and about 7.0 Btu/in.^{2}·sec in the nozzle for the 1000 psia runs, and were about 3.5 Btu/in.^{2}·sec in the combustion chamber and about 9.0 Btu/in.^{2}·sec in the nozzle for the 1500 psia runs. These heat transfer rates were about 20 per cent lower in the combustion chamber and about 10 per cent lower in the nozzle than the values obtained previously with WFNA and JP-4 in the same motors. Differences this great would be expected since the adiabatic flame temperature of acid and ammonia is about 1000°F lower than the adiabatic flame temperature of 5200°F for acid and JP-4.

The heat transfer rates in the nozzle obtained with regenerative-cooling of the nozzle were within the range of the heat transfer rates obtained with water-cooling of the nozzle. The heat transfer rate in the combustion chamber obtained with regenerative-cooling of the combustion chamber was lower than the range of heat transfer rates obtained with water-cooling of the combustion chamber, possibly indicating that more solid was deposited on the combustion chamber wall during the regeneratively-cooled run or that deposits were formed in the coolant passage.

CONCLUSIONS

1. Water-cooled rocket motors having nominal values of thrust = 500 lb, L^* = 100 in., and contraction ratio = 18, were successfully operated at combustion pressures of 1000 psia and 1500 psia using the propellant combinations WFNA-ammonia and RFNA(15% N_2O_4)-ammonia.

2. The performance and heat transfer values obtained with RFNA as the oxidizer were substantially the same as the performance and heat transfer values obtained with WFNA as the oxidizer.

3. The maximum values of the characteristic velocity, the specific impulse, and the heat transfer rates were obtained at mixture ratios (oxidizer/fuel by mass) between 2.0 and 2.3.

4. The maximum value of the characteristic velocity was 4980 ft/sec (94 per cent of theoretical) at 1000 psia combustion pressure and was 5040 ft/sec (95 per cent of theoretical) at 1500 psia combustion pressure. The maximum value of the specific impulse corrected for heat transfer was 242 $lb_f \cdot sec/lb_m$ (93 per cent of theoretical) at 1000 psia combustion pressure and was 250 $lb_f \cdot sec/lb_m$ (93 per cent of theoretical) at 1500 psia combustion pressure.

5. The maximum value of the average heat transfer rate in the combustion chamber was about 2.9 $Btu/in.^2 \cdot sec$ at 1000 psia combustion pressure and was about 3.5 $Btu/in.^2 \cdot sec$ at 1500 psia combustion pressure. The maximum value of the average heat transfer rate in the nozzle was about 7.0 $Btu/in.^2 \cdot sec$ at 1000 psia combustion pressure and was about 9.0 $Btu/in.^2 \cdot sec$ at 1500 psia combustion pressure.

6. The performance obtained with acid and ammonia was 2 to 4 per cent lower than the performance obtained with acid and JP-4 employing the same rocket motors. The heat transfer rates obtained with acid and ammonia

were 10 to 20 per cent lower than the heat transfer rates obtained with acid and JP-4.

7. The rocket motor employed in the experiments at 1000 psia combustion pressure was successfully operated with regenerative cooling; the fuel (ammonia) was utilized for cooling the nozzle and the oxidizer (RFNA) for cooling the combustion chamber. The coolant pressure drops were 800 psi in the nozzle and 400 psi in the combustion chamber.

APPENDIX A

SYMBOLS

A_t	throat area of the nozzle, $in.^2$
c^*	characteristic velocity, ft/sec
C_F	thrust coefficient
F	thrust, lb_f
I_s	specific impulse, $lb_f \cdot sec/lb_m$
I_{s_a}	specific impulse corrected to adiabatic wall conditions, $lb_f \cdot sec/lb_m$
I_{s_r}	specific impulse corrected to regeneratively-cooled conditions, $lb_f \cdot sec/lb_m$
k	apparent specific heat ratio of the combustion gases in the nozzle
L^*	ratio of the combustion chamber volume (from the injector face to the nozzle throat) to the nozzle throat area, in.
$\dot{m}_f$	flow rate of the fuel, lb_m/sec
$\dot{m}_o$	flow rate of the oxidizer, lb_m/sec
$\dot{m}_c$	flow rate of the coolant through the combustion chamber and the turbulence ring, lb_m/sec
$\dot{m}_n$	flow rate of the coolant through the nozzle, lb_m/sec
P_c	combustion pressure, psia
ΔP_{i_f}	pressure drop in the fuel injection orifices, psi
ΔP_{i_o}	pressure drop in the oxidizer injection orifices, psi
q_c	average heat transfer rate in the combustion chamber, $Btu/in.^2 \cdot sec$
q_n	average heat transfer rate in the nozzle, $Btu/in.^2 \cdot sec$
Q_c	total heat transfer rate in the combustion chamber, Btu/sec
Q_n	total heat transfer rate in the nozzle, Btu/sec
Q_{tr}	total heat transfer rate to the turbulence ring, Btu/sec
r	mixture ratio, oxidizer/fuel by mass ($r = \dot{m}_o/\dot{m}_f$)

S_c heat transfer area of the combustion chamber wall, $in.^2$

S_n heat transfer area of the nozzle wall, $in.^2$

ΔT_c temperature rise of the coolant at the outlet of the coolant passage in the combustion chamber, ^oF

ΔT_n temperature rise of the coolant at the outlet of the coolant passage in the nozzle, ^oF

ΔT_{tr} temperature rise of the coolant at the outlet of the coolant passage in the turbulence ring, ^oF

APPENDIX B

DESCRIPTION OF RESEARCH ROCKET MOTORS

1. Rocket Motor Employed for the Investigation at 1000 psia Combustion Pressure

The nozzle of the motor employed for the investigation at 1000 psia combustion pressure was the same nozzle that was employed for the investigation of WFNA and JP-4 reported in Reference 2. Due to the loss of copper from the throat of the nozzle during the WFNA - JP-4 runs the throat diameter at the beginning of the acid-ammonia investigation was 0.692 in. instead of the design value of 0.641 in. indicated in Figure 6, Reference 2. During the acid-ammonia runs the throat diameter gradually increased to about 0.698 in. The mean diameter of the throat during the runs was 0.695 in. so that the contraction ratio for the nozzle was 15.3 and the L^* of the rocket motor was 109 in.; the thrust of the rocket motor at 1000 psia combustion pressure was 580 lb. The expansion ratio of the nozzle was 7.8, making the nozzle underexpanded since the calculated expansion ratio for optimum expansion to 14.5 psia (the local mean atmospheric pressure) was 8.4; however, the calculated loss in thrust coefficient and specific impulse due to underexpansion was only 0.04 per cent. The heat transfer area of the nozzle wall was 24.0 $in.^2$. For the regeneratively-cooled runs the nozzle throat was forced outward with a tapered rod to insure complete contact with the filler block; this resulted in a throat diameter of 0.767 in., and the corresponding contraction ratio was 12.6, the L^* was 89 in., the thrust was 700 lb, and the expansion ratio of the nozzle was 6.4, making the nozzle underexpanded to the extent of a 0.4 per cent loss in thrust coefficient and specific impulse.

Water was supplied to the coolant passage of the nozzle at a pressure of approximately 1000 psia and with a flow rate of approximately 1.2 lb/sec.

The water was discharged from that coolant passage at a pressure of approximately 150 psia. For the runs utililizing ammonia for cooling the nozzle the ammonia entered the coolant passage of the nozzle at a pressure of about 2000 psia with a flow rate of about 0.91 lb/sec and the ammonia was discharged from that coolant passage at 1200 psia.

The combustion chamber was the one employed in the investigation of WFNA and JP-4 reported in Reference 2, and the turbulence ring was made to the same drawings as the turbulence ring employed in the WFNA - JP-4 investigation. The heat transfer area of the combustion chamber wall was 43.4 $in.^2$.

Water was supplied to the coolant passage of the combustion chamber at a pressure of about 800 psia and with a flow rate of about 1.4 lb/sec. The water was discharged from that coolant passage at a pressure of approximately 500 psia. The same water then entered the coolant passage in the turbulence ring and was discharged from the turbulence ring with a pressure of approximately 400 psia. For the run with acid-cooling of the combustion chamber and turbulence ring the acid entered the coolant passage of the combustion chamber at a pressure of about 1750 psia with a flow rate of 2.0 lb/sec and was discharged from that coolant passage with a pressure of approximately 1350 psia; the acid was discharged from the coolant passage of the turbulence ring at 1200 psia.

The injector was a new one having the same impingement-point locations as the injector employed in the investigation of WFNA and JP-4 reported in Reference 2. The new injector, however, had the same manifold design and the same built-in fuel valve as the injector of the motor employed for the investigation at 1500 psia combustion pressure (Cf. Figure 11). The injector orifice diameters were 0.063 in. for the fuel (6 orifices) and 0.055 in.

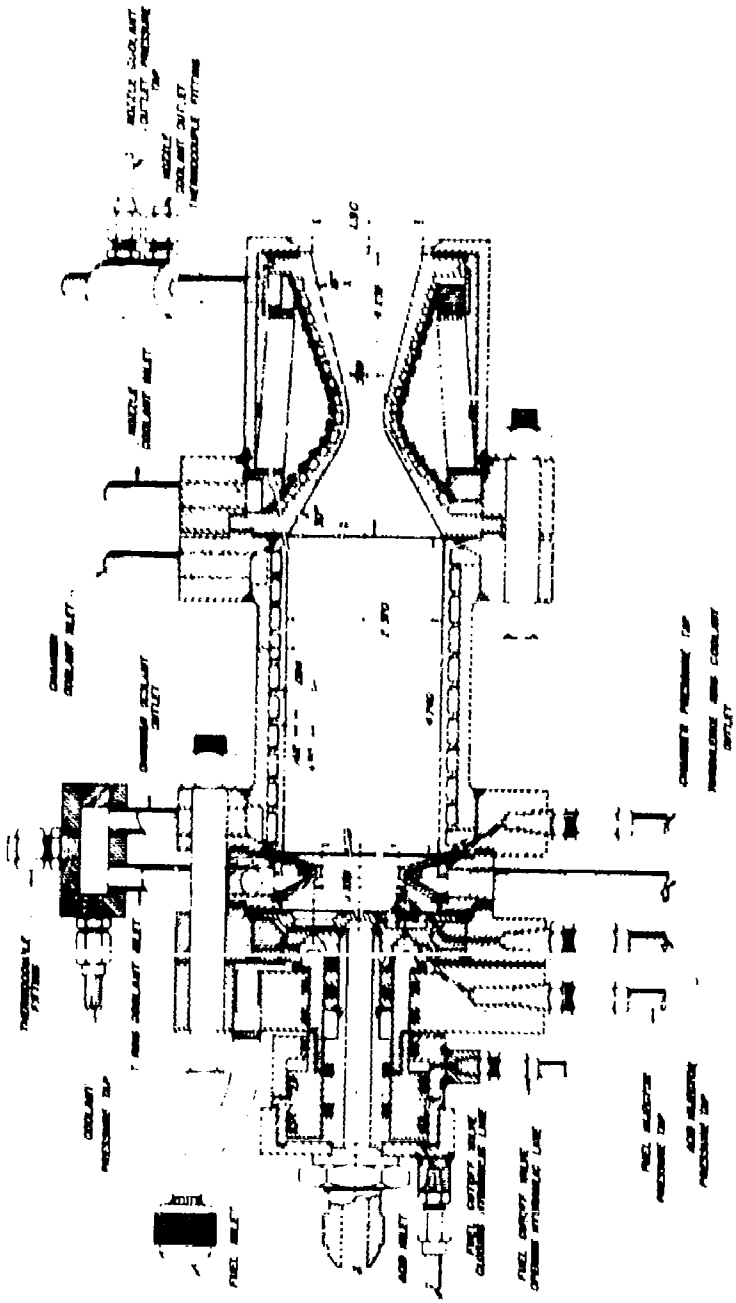

Figure 11. Cross-Section of the Research Rocket Motor Employed for the Investigation at 1500 psia Combustion Pressure

for the oxidizer (12 orifices). The ratio of the length to the diameter for the fuel orifices was 2.5 and the ratio of the length to the diameter for the oxidizer orifices was 3.1. The entrances of the oxidizer orifices were square and originally the entrances of the fuel orifices were chamfered to a diameter of 0.1 in. In water tests of the injector (with atmospheric back pressure) the fuel streams were observed to break up rapidly after leaving the injection orifices. Subsequently during the investigation of WFNA at 1000 psia combustion pressure two runs gave anomalously low performance; since the change in performance might have been due to an increase in the dispersion of the fuel streams under some flow conditions, the chamfered entrances of the fuel orifices were welded shut and redrilled to give square entrances. The experiments with RFNA were conducted with the redrilled fuel orifices and measurements showed that the pressure drop in the redrilled orifices was the same as in the original orifices. It was found later, however, that the anomalously low performance obtained in the two runs discussed above was not due to changes in the dispersion of the fuel streams but to plugging of the oxidizer orifices resulting from the use of a drum of acid containing an exceptionally large amount of suspended solids. The anomalous data were discarded.

2. Rocket Motor Employed for the Investigation at 1500 psia Combustion Pressure

Figure 11 presents a drawing of the rocket motor that was employed for the investigation at 1500 psia combustion pressure. The nozzle of that motor was the same one that was employed for the investigation of WFNA and JP-4 reported in Reference 3. Due to the loss of copper from the throat of the nozzle during the WFNA - JP-4 runs the throat diameter at the beginning of the acid-ammonia investigation was 0.555 in. instead of

the design value of 0.520 in. indicated in Figure 11. During the acid-ammonia runs the throat diameter gradually increased to about 0.563 in. and the throat became scored and out-of-round. The mean diameter of the throat during the runs was 0.559 in. so that the contraction ratio for the nozzle was 18.0 and the L^* of the rocket motor was 114 in.; the thrust of the rocket motor at 1500 psia combustion pressure was 570 lb. The expansion ratio for the nozzle was 10.4, making the nozzle under-expanded since the calculated expansion ratio for optimum expansion to 14.5 psia was 11.3; however, the calculated loss in thrust coefficient and specific impulse due to under-expansion was only 0.04 per cent. The heat transfer area of the nozzle wall was 17.9 $in.^2$.

Water was supplied to the coolant passage of the nozzle at a pressure of approximately 1500 psia and with a flow rate of approximately 1.9 lb/sec. The water was discharged from that coolant passage at a pressure of approximately 200 psia.

The combustion chamber and the turbulence ring were made to the same drawings as the combustion chamber and the turbulence ring employed in the investigation of WFNA and JP-4 reported in Reference 3. The heat transfer area of the combustion chamber wall was 35.3 $in.^2$.

Water was supplied to the coolant passage of the combustion chamber at a pressure of about 1000 psia and with a flow rate of about 1.5 lb/sec. The water was discharged from that coolant passage at a pressure of approximately 750 psia. The same water then entered the coolant passage in the turbulence ring and was discharged from the turbulence ring at a pressure of approximately 650 psia.

The injector was the injector "C" employed in the investigation of WFNA and JP-4 reported in Reference 3; the 6 fuel injection orifices were enlarged

to a diameter of 0.063 in. and the 12 oxidizer injection orifices were left at their original diameter of 0.055 in. The ratio of the length to the diameter for the fuel orifices was 2.2 and the ratio of the length to the diameter for the oxidizer orifices was 3.3.

The propellant valve employed for the investigation of acid and ammonia was that utilized in investigating WFNA and JF-4 at 1500 psia combustion pressure. Partial-flow starts were employed; one pair of propellant valves opened and admitted about one fourth of the full flow rate to the rocket motor; then, after about one second of operation at partial flow, the second pair of valves opened and the flow rates increased in a period of about 0.1 second to their full values. The starts were sometimes audibly rough, but the oscillograph records (valid to about 100 cps) showed no overshoot in the combustion pressure.

APPENDIX C

DEFINITIONS AND FORMULAS USED IN CALCULATING PERFORMANCE AND HEAT TRANSFER VALUES

The definitions used in this report for the performance parameters I_s, c^*, and C_F are as follows:*

$$I_s = \frac{F}{\dot{m}_o + \dot{m}_f} \quad lb_f \cdot sec/lb_m \tag{1}$$

$$c^* = \frac{P_c A_t}{\dot{m}_o + \dot{m}_f} \quad lb_f \cdot sec/lb_m$$

$$\text{or } c^* = 32.1739 \frac{P_c A_t}{\dot{m}_o + \dot{m}_f} \quad ft/sec \tag{2}$$

$$C_F = \frac{F}{P_c A_t} \tag{3}$$

The values of average heat transfer rate in the combustion chamber and in the nozzle were calculated from:

$$q_c = Q_c/S_c \tag{4}$$

$$q_n = Q_n/S_n \tag{5}$$

The equation used for calculating Q_c and Q_n, as well as Q_{tr}, was derived as follows:

Fluid flows through a coolant passage with mass flow rate $\dot{m}$, and between the inlet, station 1, and the outlet, station 2, heat is transferred to the passage at the rate of Q heat units per unit time. The

* For notation see Appendix A.

flow is steady, and kinetic energy changes and height changes between stations 1 and 2 can be neglected. The steady-flow energy equation gives for this case

$$Q = \dot{m} (h_2 - h_1) \tag{6}$$

where h is the enthalpy per unit mass of the fluid.

If the temperature T and the pressure P at stations 1 and 2 are measured then equation 6 can be employed directly in the form

$$Q = \dot{m} [h(T_2, P_2) - h(T_1, P_1)] \tag{7}$$

If the temperature and the pressure at station 2 are measured both with heat transfer = Q and with heat transfer = O, then Q can be calculated from equation 7 modified as follows: From equation 7, for Q = O

$$O = \dot{m} [h(T_2, P_2) - h(T_1, P_1)] \tag{8}$$

Let T_{2_o} and P_{2_o} be the values of T_2 and P_2 when Q = O and let T_{1_o} and P_{1_o} be the values of T_1 and P_1 when Q = O. From equation 8 it follows that

$$h(T_{2_o}, P_{2_o}) = h(T_{1_o}, P_{1_o})$$

But $T_{1_o} = T_1$ and $P_{1_o} = P_1$, since the entrance conditions are not affected by the rate of heat transfer. Hence

$$h(T_{2_o}, P_{2_o}) = h(T_1, P_1)$$

Substituting the last relation into equation 7 gives

$$Q = \dot{m} [h(T_2, P_2) - h(T_{2_o}, P_{2_o})]$$

For the experiments reported herein $P_2 = P_{2_o}$. Hence the last expression can be written

$$Q = \dot{m} \int_{T_{2_o}}^{T_2} c_p(P_2, T)\, dT$$

where c_p is the constant-pressure specific heat of the fluid. The last relation can be approximated by

$$Q = \dot{m}\, \overline{c_p}\, (T_2 - T_{2_o}) = \dot{m}\, \overline{c_p}\, \Delta T \qquad (9)$$

where $\overline{c_p}$ is the value of the specific heat at the pressure P_2 and at a temperature equal to $\frac{T_2 + T_{2_o}}{2}$.

Equation 9 was employed for calculating Q_c, Q_n, and Q_{tr} for the runs with water-cooling since in the interest of simplifying the instrumentation the inlet temperatures were not measured. The cooling water was allowed to flow long enough before each run to permit a constant value of T_1 to be reached, as is required for equation 9 to be valid. Equation 7 was employed for calculating the heat transfer rates for the runs with regenerative cooling since inlet temperatures were measured in those experiments.

The values of specific impulse corrected for heat transfer (I_{s_a} corrected to adiabatic wall conditions and I_{s_r} corrected to regenerative-cooling conditions) were calculated from equations derived as follows (the derivation is based on that presented in Reference 6):

A. Temperature ratio across the nozzle with heat transfer

Consider an ideal rocket motor in which a perfect gas enters the nozzle at the temperature T_c, the pressure P_c, and with the flow rate $\dot{m} = \dot{m}_o + \dot{m}_f$. The gas has specific heats c_p and c_v, gas constant $R = c_p - c_v$, and specific heat ratio $k = c_p/c_v$. The temperature and

the pressure at the nozzle exit are T_e and P_e; the pressure P_a is also equal to the atmospheric pressure. The entropy change of a unit mass of the gas as it goes from the initial state T_c and P_c to the final state T_e and P_e is given by the well-known equation

$$\Delta S_{gas} = c_p \ln \frac{T_e}{T_c} - R \ln \frac{P_e}{P_c}$$

During the change of state of the unit mass of gas an amount of heat $Q_n/\dot{m}$ is transferred to the surroundings. If the heat transfer history of the gas is specified, together with T_c, P_c, and P_e, then the final temperature of the gas T_e is determined with no additional information being needed about the gas or the surroundings. In particular, T_e does not depend on the temperature of the surroundings; the surroundings can therefore have any temperature. If the temperature of the surroundings is at each moment the same as the temperature T of the gas, then the heat is transferred reversibly to the surroundings and the entropy change of the surroundings during the change of state of the gas is given by

$$\Delta S_{surroundings} = \int_{T_c}^{T_e} \frac{d Q_n}{\dot{m} T}$$

But $\Delta S_{universe} = \Delta S_{gas} + \Delta S_{surroundings} = 0$

Hence $c_p \ln \frac{T_e}{T_c} - R \ln \frac{P_e}{P_c} + \int_{T_c}^{T_e} \frac{d Q_n}{\dot{m} T} = 0$

Define $\bar{T}$ by $$\int_{T_c}^{T_e} \frac{dQ_n}{\dot{m}T} = \frac{Q_n}{\dot{m}\bar{T}}$$

Then $$c_p \ln \frac{T_e}{T_c} = R \ln \frac{P_e}{P_c} - \frac{Q_n}{\dot{m}\bar{T}}$$

Or $$\frac{T_e}{T_c} = \left(\frac{P_e}{P_c}\right)^{\frac{R}{c_p}} e^{-\frac{Q_n}{\dot{m} c_p \bar{T}}}$$

For small values of $Q_n/\dot{m} c_p T$ the approximation can be made that

$$e^{-\frac{Q_n}{\dot{m} c_p \bar{T}}} = 1 - \frac{Q_n}{\dot{m} c_p \bar{T}}$$

This approximation was found to be accurate to within 0.2 per cent for the values of Q_n, $\dot{m}$, c_p and $\bar{T}$ encountered in the acid-ammonia investigation. Thus, the approximate value of T_e/T_c is given by the relation

$$\frac{T_e}{T_c} = \left(\frac{P_e}{P_c}\right)^{\frac{k-1}{k}} \left(1 - \frac{Q_n}{\dot{m} c_p \bar{T}}\right) \qquad (10)$$

B. Nozzle exit velocity with heat transfer

Applying the steady-flow energy equation to the flow through the nozzle gives

$$-Q_n = \dot{m}(h_e - h_c) + 1/2\, \dot{m} V^2$$

where

h_c = the specific enthalpy of the gas at the entrance of the nozzle

h_e = the specific enthalpy of the gas at the exit of the nozzle

V = the velocity of the gas at the exit of the nozzle

(The velocity of the gas at the entrance of the nozzle is assumed to be zero)

Thus $1/2\ \dot{m}\ V^2 = \dot{m}\ c_p\ (T_c - T_e) - Q_n$

Or $$\frac{V^2}{2} = c_p\ T_c\ \left(1 - \frac{T_e}{T_c} - \frac{Q_n}{\dot{m}\ c_p\ T_c}\right) \qquad (11)$$

Substituting T_e/T_c from equation 10 yields

$$\frac{V^2}{2} = c_p\ T_c \left\{ 1 - \left(\frac{P_e}{P_c}\right)^{\frac{k-1}{k}} - \frac{Q_n}{\dot{m}\ c_p\ T_c} \left[1 - \frac{T_c}{\overline{T}} \left(\frac{P_e}{P_c}\right)^{\frac{k-1}{k}} \right] \right\} \qquad (12)$$

C. Temperature of the gas entering the nozzle

The enthalpy of the gas entering the nozzle is equal to the enthalpy for adiabatic combustion $c_p T_{c_a}$ (based upon the propellants entering the combustion chamber at some standard temperature) plus any enthalpy added to the propellants by regenerative cooling of the combustion chamber, turbulence ring, and nozzle, minus any enthalpy taken from the gas by heat transfer to the combustion chamber and to the turbulence ring. (Subscript "a" indicates adiabatic conditions, subscript "r" indicates conditions for regenerative-cooling, and subscript "w" indicates conditions for water-cooling). Thus the enthalpy of the gas entering the nozzle for the adiabatic case (no heat transfer to the chamber, nozzle, or turbulence ring) is

$$\dot{m}\ h_{c_a} = \dot{m}\ c_p\ T_{c_a} \qquad (13)$$

The enthalpy of the gas entering the nozzle for the water-cooled case ($Q_c + Q_{tr}$ transferred from the gas to the cooling water in the combustion chamber and the turbulence ring and Q_n transferred from

the gas to the cooling water in the nozzle) is

$$\dot{m}\, h_{c_w} = \dot{m}\, c_p\, T_{c_w} = \dot{m}\, c_p\, T_{c_a} - (Q_c + Q_{tr}) \tag{14}$$

The enthalpy of the gas entering the nozzle for the regeneratively-cooled case ($Q_c + Q_{tr}$ transferred from the gas to the propellant used for cooling the chamber and the turbulence ring and Q_n transferred from the gas to the propellant used for cooling the nozzle) is

$$\dot{m}\, h_{c_r} = \dot{m}\, c_p\, T_{c_r} = \dot{m}\, c_p\, T_{c_a} - (Q_c + Q_{tr}) + (Q_c + Q_{tr} + Q_n)$$

$$= \dot{m}\, c_p\, T_{c_a} + Q_n \tag{15}$$

From equation 15

$$T_{c_a} = T_{c_r} - \frac{Q_n}{\dot{m}\, c_p} \tag{16}$$

Combining equations 14 and 16 gives

$$T_{c_w} = T_{c_r} - \frac{Q_c + Q_{tr} + Q_n}{\dot{m}\, c_p} \tag{17}$$

D. Nozzle exit velocity with water cooling

Substituting $T_c = T_{c_w}$ in equation 12 and using the value of T_{c_w} from equation 17 gives

$$\frac{V_w^2}{2} = c_p\, T_{c_r} \left(1 - \frac{Q_c + Q_{tr} + Q_n}{\dot{m}\, c_p\, T_{c_r}}\right) \times$$

$$\left\{1 - \left(\frac{P_e}{P_c}\right)^{\frac{k-1}{k}} - \frac{Q_n}{\dot{m}\, c_p\, T_{c_r} \left(1 - \frac{Q_c + Q_{tr} + Q_n}{\dot{m}\, c_p\, T_{c_r}}\right)} \left[1 - \lambda \left(\frac{P_e}{P_c}\right)^{\frac{k-1}{k}}\right]\right\} \tag{18}$$

where $\lambda = T_{c_w}/\bar{T}_w$

E. Nozzle exit velocity with regenerative cooling

Substituting $T_c = T_{c_r}$ in equation 12 and assuming that $T_{c_r}/T_r = T_{c_w}/T_w$ (calculated to be correct within 0.5 per cent for the acid-ammonia experiments) gives

$$\frac{V_r^2}{2} = c_p T_{c_r} \left\{ 1 - \left(\frac{P_e}{P_c}\right)^{\frac{k-1}{k}} - \frac{Q_n}{\dot{m} c_p T_{c_r}} \left[1 - \lambda \left(\frac{P_e}{P_c}\right)^{\frac{k-1}{k}} \right] \right\} \qquad (19)$$

F. Nozzle exit velocity with no heat transfer (adiabatic conditions)

Substituting $T_c = T_{c_a}$ in equation 12, (with $Q_n = 0$) and using the value of T_{c_a} from equation 16, gives

$$\frac{V_a^2}{2} = c_p T_{c_r} \left(1 - \frac{Q_n}{\dot{m} c_p T_{c_r}}\right) \left[1 - \left(\frac{P_e}{P_c}\right)^{\frac{k-1}{k}} \right] \qquad (20)$$

G. Equations for I_{s_r} and I_{s_a}

Eliminating $c_p T_{c_r}$ between equations 18 and 19 yields

$$\frac{V_r^2}{2} = \frac{V_w^2}{2} + \frac{Q_c + Q_{tr} + Q_n}{\dot{m}} \left[1 - \left(\frac{P_e}{P_c}\right)^{\frac{k-1}{k}} \right]$$

or since $V = F/\dot{m} = I_s$,

$$I_{s_r} = \sqrt{I_{s_w}^2 + 2 \frac{Q_c + Q_{tr} + Q_n}{\dot{m}} \left[1 - \left(\frac{P_e}{P_c}\right)^{\frac{k-1}{k}} \right]} \qquad (21)$$

Eliminating $c_p T_{c_r}$ between equations 19 and 20 yields

$$\frac{V_a^2}{2} = \frac{V_r^2}{2} - \frac{Q_n}{\dot{m}} (\lambda - 1) \left(\frac{P_e}{P_c}\right)^{\frac{k-1}{k}}$$

$$\text{or } I_{s_a} = \sqrt{I_{s_r}^2 - \frac{Q_n}{\dot{m}} (\lambda - 1) \left(\frac{P_e}{P_c}\right)^{\frac{k-1}{k}}} \tag{22}$$

The value of λ employed for the acid-ammonia investigation was 1.312; this value of λ corresponded to a heat transfer distribution calculated for the 1500 psia nozzle with WFNA and JP-4 as the propellants. For $\lambda = 1.312$, and for the units of I_s, Q, and $\dot{m}$ listed in Appendix A, equations 21 and 22 become:

$$I_{s_r} = \sqrt{I_{s_w}^2 + 48.378 \frac{Q_c + Q_{tr} + Q_n}{\dot{m}_o + \dot{m}_f} \left[1 - \left(\frac{P_e}{P_c}\right)^{\frac{k-1}{k}}\right]} \tag{23}$$

$$I_{s_a} = \sqrt{I_{s_r}^2 - 15.11 \frac{Q_n}{\dot{m}_o + \dot{m}_f} \left(\frac{P_e}{P_c}\right)^{\frac{k-1}{k}}} \tag{24}$$

The value of k used for the acid-ammonia investigation was 1.23. The maximum difference between I_{s_r} and I_{s_w} for the acid-ammonia experiments was 7.4 $lb_f \cdot sec/lb_m$ and the maximum difference between I_{s_r} and I_{s_a} was 0.9 $lb_f \cdot sec/lb_m$; since the value used for λ was only approximate for the acid-ammonia experiments, the latter difference could be as little as 0.5 $lb_f \cdot sec/lb_m$ or as large as 1.5 $lb_f \cdot sec/lb_m$ for the estimated uncertainty in λ.

APPENDIX D

EXTRAPOLATION OF THEORETICAL PERFORMANCE VALUES TO 1000 PSIA AND 1500 PSIA COMBUSTION PRESSURES

The theoretical performance values presented in Figures 1 through 7 for comparison with the measured performance values were obtained by extrapolating the theoretical values of performance based upon thermochemical calculations for HNO_3 and NH_3 presented in Reference 5. The latter reference presents theoretical (frozen composition) values of I_s and c^* as a function of mixture ratio for combustion pressures of 300, 400, 500, 600, 700, and 800 psia, based on an exit pressure of 14.7 psia; the mixture ratios covered are 1.0 to 3.0 mole ratio of NH_3 to HNO_3, which correspond to mixture ratios of HNO_3 to NH_3 by mass of 3.70 to 1.23.

The values of theoretical c^* were extrapolated to combustion pressures of 1000 psia and 1500 psia by plotting the values of c^* from Reference 5 as a function of combustion pressure from 300 psia to 800 psia and by extending the curves by free-hand to 1500 psia. Since the theoretical values of c^* increase by no more than 0.07 per cent per 100 psi at 800 psia combustion pressure it was estimated that the maximum error in the extrapolated values of c^* is 0.2 per cent. The extrapolated values of c^* are presented in Table 2.

The values of C_F at 1000 psia and 1500 psia combustion pressure were calculated, employing extrapolated values of k, by means of the equation for the thrust coefficient of an ideal jet motor which is

$$C_F = \sqrt{\frac{2k^2}{k-1}\left(\frac{2}{k+1}\right)^{\frac{k+1}{k-1}}\left[1-\left(\frac{P_e}{P_c}\right)^{\frac{k-1}{k}}\right]} \qquad (1)$$

The values of k used at 1000 psia and 1500 psia combustion pressure were extrapolated for each mixture ratio from a plot of k as a function of combustion pressure from 300 psia through 800 psia. The values of k at 300 psia through 800 psia combustion pressure were obtained by (1) plotting curves of C_F as a function of k, employing equation 1, for values of P_e/P_c corresponding to P_c = 300, 400, 500, 600, 700, and 800 psia and P_e = 14.7 psia and (2) reading the values of k corresponding to the values of C_F (= 32.174 I_s/c^*) given in Reference 5. The maximum variation of k with pressure was found to lead to a maximum uncertainty in the extrapolated values of k of about 0.3%; the corresponding maximum error in C_F is 0.15%. The values of extrapolated C_F and k are presented in Tables 2 and 3.

The values of theoretical I_s at combustion pressures of 1000 psia and 1500 psia were calculated from the extrapolated values of c^* and C_F by means of the relation $I_s = C_F c^*/32.174$. The maximum error in I_s, combining the extrapolation errors of c^* and C_F is approximately 0.35%. The values of extrapolated I_s are presented in Table 2.

TABLE 2

Theoretical (Frozen Composition) Performance of HNO_3 and NH_3

Extrapolated from Reference 5

r	Performance at 1000 psia combustion pressure			Performance at 1500 psia combustion pressure		
	I_s	c^*	C_F	I_s	c^*	C_F
1.233	237.2	4911	1.554	244.1	4911	1.599
1.321	241.5	4986	1.558	248.5	4986	1.604
1.423	245.8	5060	1.563	253.2	5061	1.610
1.542	250.0	5131	1.567	257.6	5133	1.615
1.682	254.0	5199	1.572	261.8	5202	1.619
1.850	257.6	5260	1.576	265.6	5265	1.623
2.056	260.1	5299	1.579	268.5	5311	1.626
2.312	256.4	5219	1.581	264.8	5232	1.628
2.643	246.2	5018	1.579	254.0	5027	1.626
3.083	233.5	4770	1.575	240.5	4773	1.621
3.700	218.2	4471	1.570	224.6	4473	1.616

TABLE 3

Theoretical (Frozen Composition) Values of Apparent Specific

Heat Ratio k Extrapolated from Reference 5

r	Values of k at 1000 psia combustion pressure	Values of k at 1500 psia combustion pressure
1.233	1.289	1.284
1.321	1.279	1.274
1.423	1.268	1.263
1.542	1.258	1.253
1.682	1.248	1.245
1.850	1.240	1.238
2.056	1.233	1.233
2.312	1.230	1.230
2.643	1.234	1.234
3.083	1.242	1.242
3.700	1.252	1.252

APPENDIX E

TABULATED PERFORMANCE AND HEAT TRANSFER DATA

Tables 4 through 7 present the experimental performance and heat transfer data which were obtained from all of the runs in which valid measurements were made. Runs for which data are not presented in Tables 4 through 7 either were runs conducted for other purposes than the program reported herein or were runs during which a malfunction prevented the measurement of valid data. The values presented in Tables 4 through 7 were rounded off from the values computed by the Datatron digital computer.

TABLE 4

Experimental Data at 1000 psia Combustion Pressure with WFNA as the Oxidizer

TABLE 4

Experimental Data at 1000 psia Combustion Pressure with WFNA as the Oxidizer

Run No.	Date	Time from start, sec	P_c, psia	F, lb_f	$\dot{m}_o$, $\frac{lb_m}{sec}$	$\dot{m}_f$, $\frac{lb_m}{sec}$	r	I_s, $\frac{lb_f \cdot sec}{lb_m}$	I_{s_r}, $\frac{lb_f \cdot sec}{lb_m}$	I_a, $\frac{lb_f \cdot sec}{lb_m}$	c^*, $\frac{ft}{sec}$	C_F	$\dot{m}_n$, $\frac{lb_m}{sec}$	$\dot{m}_c$, $\frac{lb_m}{sec}$	ΔT_n, °F	ΔT_c, °F	ΔT_{tr}, °F	q_n, $\frac{Btu}{in^2 \cdot sec}$	q_c, $\frac{Btu}{in^2 \cdot sec}$	Q_{tr}, $\frac{Btu}{sec}$
262	9- 7-55	35-40	1012	585.7	1.622	0.958	1.692	227.0	232.9	232.1	4743	1.540	1.020	1.354	127.0	81.6	16.0	5.44	2.50	21.6
263	10-15-55	15-25	1063	618.4	1.837	0.812	2.263	233.5	239.0	238.2	4866	1.544	1.044	1.493	143.1	68.1	6.5	6.29	2.30	9.7
		35-40	993	574.9	1.916	0.698	2.744	219.9	224.9	224.2	4607	1.536	1.069	1.502	120.4	54.2	8.3	5.41	1.84	12.3
		45-50	1035	603.6	1.870	0.763	2.452	229.3	234.6	233.8	4768	1.547	1.064	1.502	132.5	60.0	8.0	5.93	2.04	11.9
		55-65	1062	621.9	1.836	0.811	2.262	234.9	240.5	239.7	4866	1.553	1.060	1.520	143.5	65.9	8.5	6.40	2.27	12.8
		77-85	1084	635.5	1.810	0.873	2.074	236.9	242.8	242.0	4903	1.555	1.053	1.537	151.1	72.7	9.9	6.69	2.53	15.1
		95-100	1086	637.1	1.798	0.890	2.021	237.0	242.9	242.1	4899	1.556	1.055	1.553	149.8	72.4	9.8	6.65	2.54	15.1
		105-120	1087	636.9	1.792	0.906	1.977	236.0	241.9	241.1	4887	1.554	1.055	1.547	147.7	72.0	10.7	6.56	2.52	16.4
267	10-28-55	15-20	1014	587.1	1.619	0.921	1.758	231.2	236.9	236.1	4862	1.530	1.114	1.466	130.6	72.5	3.4	6.04	2.44	4.9
		35-40	1002	580.7	1.588	0.936	1.696	230.1	235.7	234.9	4839	1.530	1.125	1.473	121.5	70.8	7.0	5.68	2.39	10.3
		45-50	991	573.0	1.540	1.010	1.525	224.7	230.2	229.4	4735	1.527	1.134	1.475	113.6	67.1	9.6	5.35	2.27	14.1
		55-65	996	576.7	1.519	1.121	1.355	218.5	223.7	223.0	4596	1.530	1.141	1.480	108.8	60.9	10.8	5.16	2.07	15.9
		75-80	980	568.8	1.442	1.304	1.106	207.1	211.9	211.3	4350	1.532	1.158	1.492	99.1	51.7	11.7	4.77	1.77	17.4
		85-90	987	574.7	1.442	1.363	1.058	204.9	209.4	208.8	4288	1.537	1.165	1.492	94.7	50.3	10.4	4.58	1.72	15.4
268	12-1 -55	13-17	1045	608.2	1.823	0.782	2.331	233.5	239.6	238.7	4935	1.523	1.063	1.472	151.5	70.8	11.0	6.70	2.39	16.1
		35-45	1066	623.1	1.992	0.760	2.620	226.4	231.7	230.9	4764	1.529	1.082	1.430	133.4	61.9	10.6	6.00	2.03	15.2
		48-51	1105	650.2	1.926	0.829	2.323	235.9	241.7	240.0	4930	1.540	1.082	1.429	151.0	72.4	12.0	6.80	2.37	17.1
		53-57	1084	636.9	1.780	0.860	2.093	239.5	245.8	244.9	5012	1.537	1.082	1.424	157.8	83.9	13.4	7.10	2.64	19.0
		70-75	1089	640.9	1.777	0.909	1.954	238.6	245.2	244.3	4985	1.540	1.082	1.430	161.5	88.4	13.6	7.27	2.90	19.3
		80-85	1097	644.2	1.766	0.965	1.830	235.9	242.4	241.6	4937	1.537	1.082	1.435	158.6	88.9	13.6	7.14	2.93	19.5
		90-95	1138	671.7	1.883	0.912	2.066	240.3	246.9	246.0	5005	1.545	1.082	1.431	168.5	90.8	15.2	7.59	2.98	21.7
		100-105	1086	637.8	1.944	0.794	2.449	232.9	239.2	238.3	4876	1.537	1.085	1.436	155.8	81.1	12.6	7.03	2.67	18.0
		108-112	1044	608.9	1.990	0.736	2.705	223.4	229.3	228.5	4709	1.527	1.091	1.445	140.1	72.4	11.4	6.36	2.40	16.4
		113-117	1045	609.8	2.035	0.727	2.797	220.8	226.4	225.6	4653	1.527	1.098	1.446	135.0	69.4	10.3	6.16	2.30	14.8
		118-120	1075	629.4	2.003	0.764	2.623	227.5	233.4	232.5	4777	1.532	1.097	1.441	144.6	73.5	11.2	6.60	2.43	16.1

CONFIDENTIAL

TABLE 5

Experimental Data at 1500 psia Combustion Pressure with WFNA as the Oxidizer

Run No.	Date	Time from start sec	P_c psia	F lb_f	$\dot{w}_o$ $\frac{lb_m}{sec}$	$\dot{w}_f$ $\frac{lb_m}{sec}$	r	I_o $\frac{lb_f \cdot sec}{lb_m}$	I_{s_f} $\frac{lb_f \cdot sec}{lb_m}$	I_{s_a} $\frac{lb_f \cdot sec}{lb_m}$	c^* ft/sec	C_F	$\dot{w}_a$ $\frac{lb_m}{sec}$	$\dot{w}_c$ $\frac{lb_m}{sec}$	ΔT_a °F	$\angle T_c$ °F	ΔT_{tr} °F	q_a $\frac{Btu}{in^2 \cdot sec}$	q_c $\frac{Btu}{in^2 \cdot sec}$	Q_{tr} $\frac{Btu}{sec}$
275	2-11-56	5-10	1531	576.3	1.601	0.744	2.151	245.7	251.9	251.1	5087	1.554	1.782	1.340	84.0	70.1	11.3	8.23	2.65	15.7
		15-20	1531	578.0	1.607	0.728	2.206	247.5	253.8	253.0	5111	1.558	1.769	1.347	84.7	71.3	11.9	8.33	2.71	16.0
		30-35	1505	560.5	1.635	0.680	2.404	244.8	251.3	250.5	5068	1.554	1.784	1.360	85.5	72.0	12.1	8.46	2.76	16.3
		48-52	1472	553.1	1.931	0.617	3.131	217.1	223.2	222.4	4505	1.551	1.791	1.384	77.5	64.1	12.1	7.73	2.50	16.7
		60-65	1495	561.0	1.809	0.640	2.827	229.1	235.5	234.6	4757	1.549	1.802	1.389	83..	67.7	11.6	8.33	2.65	16.0
		80-90	1464	548.0	2.035	0.599	3.394	208.0	213.8	213.0	4332	1.545	1.816	1.404	71.9	59.2	10.0	7.26	2.34	14.0
		100-105	1492	558.0	1.988	0.619	3.212	214.0	219.9	219.2	4459	1.544	1.821	1.405	72.0	63.4	11.0	7.39	2.51	15.4
		120-135	1489	560.0	1.596	0.690	2.311	245.0	252.2	251.3	5077	1.553	1.820	1.380	87.2	86.1	11.7	8.82	3.35	16.1
		147-150	1508	569.3	1.537	0.766	2.008	247.3	254.7	253.8	5105	1.558	1.825	1.383	90.6	91.5	11.4	9.20	3.56	15.7
276	2-13-56	5-10	1460	549.0	1.473	0.802	1.836	241.2	247.3	246.5	4989	1.556	1.768	1.352	77.9	67.2	10.5	7.66	2.56	14.1
		15-25	1486	560.0	1.508	0.766	1.968	246.1	252.8	251.9	5083	1.559	1.776	1.360	85.8	73.8	11.9	8.47	2.83	16.2
		40-45	1495	565.5	1.610	0.690	2.334	246.0	253.0	252.1	5057	1.565	1.783	1.370	90.4	82.0	12.1	8.97	3.16	16.5
		65-80	1500	56..4	1.932	0.627	3.083	219.6	225.3	224.6	4595	1.548	1.801	1.408	76.1	62.7	10.1	7.42	2.69	15.5
		115-130	1488	549.1	2.021	0.600	3.366	209.5	214.5	213.8	4413	1.527	1.817	1.492	63.5	49.1	8.3	6.41	2.02	12.0
		135-150	1489	548.2	2.020	0.600	3.369	209.2	214.2	213.6	4421	1.523	1.818	1.451	60.7	50.5	9.0	6.13	2.06	13.0
277	2-13-56	22-27	1508	571.7	1.596	0.698	2.285	249.3	256.3	255.4	5161	1.560	1.775	1.352	89.4	84.7	12.6	8.83	3.23	17.0
		30-35	1535	580.0	1.527	0.824	1.865	245.7	252.2	251.4	5087	1.554	1.775	1.357	85.2	76.6	11.2	8.41	2.93	15.1
		45-50	1506	568.3	1.487	0.856	1.738	242.6	248.6	247.9	5027	1.552	1.782	1.367	79.4	67.5	12.2	7.87	2.60	16.5
		65-80	1502	568.0	1.426	1.043	1.367	230.0	235.6	234.7	4758	1.556	1.785	1.401	73.0	53.9	11.0	7.24	2.13	15.3
		85-90	1469	555.6	1.381	1.087	1.294	228.9	232.1	231.4	4693	1.556	1.784	1.414	69.4	50.5	10.8	6.89	2.01	15.1
		95-110	1504	568.3	1.432	1.019	1.405	231.9	237.2	236.5	4800	1.554	1.782	1.405	72.2	53.5	10.6	7.15	2.12	14.8
278	2-14-56	18-22	1501	562.7	1.406	1.158	1.214	219.4	224.4	223.8	4592	1.538	1.796	1.391	65.6	50.6	11.6	6.55	1.98	16.1
		25-40	1502	562.0	1.391	1.183	1.176	218.4	223.3	222.6	4570	1.538	1.801	1.408	66.0	46.0	11.3	6.61	1.82	15.8
		45-55	1491	560.0	1.387	1.173	1.182	218.8	223.7	223.0	4568	1.541	1.806	1.415	68.4	43.5	10.3	6.87	1.73	14.5
		63-67	1534	579.4	1.461	1.107	1.319	225.6	230.7	230.0	4682	1.550	1.812	1.407	75.5	46.1	9.8	7.61	1.83	13.7
		75-80	1507	569.1	1.431	1.096	1.307	225.2	230.6	229.8	4677	1.550	1.815	1.413	77.9	48.5	10.1	7.86	1.85	14.2
		85-95	1499	566.0	1.460	0.973	1.501	232.7	238.5	237.7	4833	1.549	1.817	1.395	83.9	52.3	9.9	8.48	2.06	13.7
279	2-16-56	10-25	1488	569.0	1.537	0.783	1.964	245.3	251.6	250.8	5042	1.566	1.802	1.362	79.1	74.2	11.7	7.92	2.85	15.9
		58-62	1503	573.4	1.943	0.651	2.984	222.0	226.4	225.7	4552	1.563	1.825	1.420	69.7	57.0	9.9	7.08	2.28	14.0
		65-75	1503	574.4	1.976	0.650	3.041	218.8	223.8	223.1	4497	1.565	1.829	1.432	65.8	51.0	9.7	6.69	2.06	13.8
		78-82	1500	574.9	2.003	0.648	3.092	216.8	221.5	220.9	4445	1.570	1.832	1.442	61.6	48.5	9.2	6.28	1.97	13.2
		90-105	1459	575.5	2.038	0.642	3.173	2.4.8	219.3	218.7	4396	1.572	1.834	1.442	58.8	46.7	9.2	6.06	1.90	1. 1
		120-135	1503	575.5	1.832	0.665	2.754	240.4	235.3	234.7	4728	1.568	1.835	1.417	61.2	55.1	10.5	6.24	2.20	14.7

Experimental Data at 1500 psia Combustion Pressure with RFNA as the Oxidizer

Run No.	Date	Time from start sec	Pc psia	F lb_f	$\dot{m}_o$ $\frac{lb_m}{sec}$	$\dot{m}_f$ $\frac{lb_m}{sec}$	r	I_s $\frac{lb_f \cdot sec}{lb_m}$	I_{s_r} $\frac{lb_f \cdot sec}{lb_m}$	I_{s_a} $\frac{lb_f \cdot sec}{lb_m}$	c^* $\frac{ft}{sec}$	C_F	$\dot{m}_n$ $\frac{lb_m}{sec}$	$\dot{m}_c$ $\frac{lb_m}{sec}$	ΔT_n °F	ΔT_c °F	ΔT_{tr} °F	q_n $\frac{Btu}{in^2 \cdot sec}$	q_c $\frac{Btu}{in^2 \cdot sec}$	Q_{tr} $\frac{Btu}{sec}$
282	3-19-56	15-25	1531	582.7	1.615	0.775	2.083	243.8	249.8	249.0	5054	1.552	1.836	1.414	75.7	70.1	10.0	7.73	2.79	14.1
		30-35	1534	581.9	1.610	0.779	2.067	243.5	249.5	248.8	5066	1.547	1.845	1.430	75.4	69.0	10.0	7.73	2.78	14.2
		40-50	1493	564.9	1.689	0.678	2.493	238.7	244.7	243.9	4976	1.544	1.848	1.451	74.9	64.6	10.0	7.70	2.64	14.4
		55-65	1503	567.5	1.679	0.684	2.454	240.2	246.2	245.4	5017	1.540	1.850	1.464	75.1	63.8	10.0	7.72	2.63	14.6
		80-90	1504	562.8	2.024	0.620	3.267	212.8	217.8	217.2	4488	1.525	1.859	1.512	61.8	46.8	10.0	6.39	1.99	15.0
		95-105	1477	550.9	2.056	0.601	3.420	207.3	212.0	211.4	4384	1.521	1.860	1.523	57.2	43.5	10.0	5.92	1.87	15.1
		115-120	1500	560.3	2.063	0.612	3.370	209.4	213.9	213.4	4423	1.523	1.861	1.526	54.6	42.7	10.0	5.65	1.84	15.2
		130-140	1536	575.6	1.983	0.640	3.098	219.5	223.9	223.3	4621	1.528	1.859	1.525	54.8	43.4	10.0	5.66	1.86	15.2
		145-155	1514	565.4	2.000	0.625	3.200	215.4	219.7	219.1	4551	1.522	1.858	1.527	50.8	41.5	10.0	5.25	1.79	15.2
283	3-20-56	25-35	1521	580.9	1.573	0.803	1.960	244.5	250.8	250.0	5080	1.549	1.893	1.455	77.3	64.6	10.4	8.14	2.65	15.1
		55-65	1513	575.1	1.768	0.686	2.577	234.4	240.3	239.5	4891	1.540	1.902	1.496	76.3	56.0	9.7	8.07	2.36	14.4
		80-90	1515	570.6	2.020	0.636	3.175	214.9	220.1	219.5	4525	1.528	1.910	1.521	64.1	51.6	8.8	6.81	2.21	13.4
		98-102	1480	556.2	2.056	0.616	3.339	208.2	213.3	212.6	4398	1.524	1.910	1.530	58.0	50.3	8.9	6.16	2.17	13.5
		113-117	1545	585.6	2.088	0.654	3.194	213.6	218.5	217.9	4472	1.537	1.907	1.531	60.0	50.3	8.5	6.36	2.17	12.9
		135-140	1496	566.4	2.062	0.628	3.281	210.5	215.3	214.7	4411	1.535	1.927	1.538	56.3	47.0	8.0	6.03	2.34	12.2
		145-150	1504	570.1	2.035	0.642	3.169	213.0	217.7	217.1	4459	1.536	1.924	1.539	55.5	45.8	9.2	5.94	1.99	14.1
285	3-27-56	10-25	1490	573.5	1.548	0.833	1.860	240.9	246.9	246.1	4982	1.556	1.850	1.419	77.8	65.6	8.7	8.05	2.02	12.3
		40-50	1497	579.4	1.655	0.721	2.295	243.8	250.5	249.7	5016	1.564	1.861	1.416	84.4	76.9	9.7	8.74	3.07	13.7
		65-75	1488	572.9	1.909	0.644	2.962	224.4	230.1	229.4	4638	1.557	1.873	1.456	71.6	61.1	8.7	7.46	2.51	12.6
		120-130	1481	567.8	2.069	0.622	3.324	211.0	215.6	215.0	4381	1.549	1.877	1.498	56.8	47.8	7.9	5.93	2.02	11.8
		140-150	1493	577.2	1.646	0.701	2.347	245.9	251.8	251.0	5064	1.563	1.877	1.451	71.6	67.5	8.1	7.48	2.76	11.7
286	3-30-56	15-56	1490	573.8	1.542	0.884	1.744	236.5	242.6	241.8	4892	1.555	1.867	1.409	78.7	67.6	10.4	8.17	2.68	14.6
		30-35	1513	586.3	1.476	1.162	1.269	222.3	227.5	226.8	4572	1.564	1.883	1.481	66.7	53.0	11.7	6.98	2.21	17.2
		75-85	1504	581.5	1.491	1.058	1.410	228.2	234.1	233.3	4701	1.561	1.893	1.479	75.7	60.8	11.0	7.97	2.54	16.2
		90-100	1493	576.8	1.523	0.916	1.662	236.4	242.9	242.1	4877	1.560	1.894	1.474	82.2	68.4	10.4	8.66	2.84	15.3
		105-110	1496	577.2	1.522	0.916	1.661	236.7	243.1	242.3	4886	1.559	1.894	1.479	80.7	68.1	10.8	8.49	2.83	15.8
287	4- 5-56	48-52	1498	587.1	1.429	1.355	1.055	210.9	216.0	215.4	4300	1.578	1.901	1.515	63.4	51.5	12.8	5.70	2.20	19.3
		55-60	1498	587.8	1.425	1.365	1.044	210.7	215.7	215.1	4291	1.580	1.901	1.518	62.6	50.0	12.6	6.61	2.14	19.0
		70-85	1490	583.8	1.433	1.288	1.113	214.5	219.6	219.0	4376	1.578	1.905	1.523	62.5	50.3	12.4	6.62	2.16	18.8
		95-100	1494	584.4	1.463	1.180	1.240	221.0	226.2	225.5	4516	1.575	1.912	1.524	62.4	52.7	11.3	6.64	2.26	17.1
288	5- 7-56	30-50	1498	596.9	1.705	0.752	2.269	243.0	249.9	249.0	4999	1.564	1.887	1.394	87.3	38.6	6.7	9.16	3.48	9.3
		65-75	1484	590.2	1.773	0.713	2.489	237.4	243.9	243.1	4896	1.560	1.895	1.416	81.3	82.4	6.7	8.57	3.29	9.5
		90-95	1484	588.5	1.918	0.683	2.808	226.3	232.2	231.5	4679	1.556	1.899	1.450	74.1	71.5	6.7	7.83	2.92	9.7
		100-105	1467	579.6	1.923	0.668	2.880	223.8	229.6	228.9	4645	1.550	1.902	1.459	71.2	69.3	6.7	7.53	2.85	9.7

CONFIDENTIAL

TABLE 7

Experimental Data at 1000 psia Combustion Pressure with RFNA as the Oxidizer

Run No.	Date	Time from start sec	P_c psia	F lb_f	$\dot{m}_o$ $\frac{lb_m}{sec}$	$\dot{m}_f$ $\frac{lb_m}{sec}$	r	I_s $\frac{lb_f \cdot sec}{lb_m}$	I_{s_r} $\frac{lb_f \cdot sec}{lb_m}$	I_{s_a} $\frac{lb_f \cdot sec}{lb_m}$	c^* $\frac{ft}{sec}$	C_F	$\dot{m}_n$ $\frac{lb_m}{sec}$	$\dot{m}_c$ $\frac{lb_m}{sec}$	ΔT_n °F	ΔT_c °F	ΔT_{tr} °F	q_n $\frac{Btu}{in^2 \cdot sec}$	q_c $\frac{Btu}{in^2 \cdot sec}$	Q_{tr} $\frac{Btu}{sec}$
291	6-21-56	15-20	1005	587.5	1.605	0.890	1.803	235.5	241.9	241.0	4944	1.532	1.169	1.375	132.6	84.7	13.4	6.45	2.67	18.4
		30-40	1009	591.3	1.627	0.853	1.908	238.4	244.6	243.8	4990	1.537	1.157	1.407	129.5	81.0	13.2	6.24	2.61	18.5
		50-60	1003	588.6	1.641	0.812	2.021	240.0	246.1	245.2	5020	1.538	1.160	1.408	127.1	78.1	12.4	6.14	2.52	17.5
		65-80	1002	586.4	1.708	0.749	2.282	238.7	244.6	243.8	5002	1.535	1.157	1.413	126.0	73.1	11.2	6.07	2.37	15.8
		95-110	1002	583.1	2.026	0.674	3.004	216.0	220.6	220.0	4554	1.526	1.194	1.431	95.8	56.1	8.5	4.76	1.85	12.1
292	6-22-56	15-25	1001	582.5	1.606	0.904	1.776	232.0	238.2	237.3	4888	1.527	1.183	1.389	129.3	76.0	13.2	6.37	2.42	18.3
		35-40	1002	584.2	1.621	0.879	1.844	233.7	239.6	238.8	4914	1.530	1.186	1.397	122.2	73.7	13.4	6.03	2.36	18.6
		55-65	1007	586.2	1.650	0.842	1.959	235.2	241.0	240.2	4952	1.528	1.190	1.407	119.3	70.7	12.8	5.91	2.28	18.0
		80-95	1002	583.8	1.660	0.816	2.035	235.8	241.4	240.6	4964	1.529	1.194	1.414	115.1	67.6	12.[illegible]	5.72	2.19	17.9
		105-120	1001	581.3	1.747	0.749	2.331	232.9	238.2	237.4	4916	1.524	1.204	1.435	110.5	60.0	11.2	5.54	1.98	16.0
293	6-25-56	15-25	1011	588.4	1.619	0.914	1.772	232.3	238.3	237.4	4890	1.528	1.206	1.384	122.9	76.7	11.7	6.17	2.43	16.2
		35-45	1011	588.9	1.642	0.870	1.886	234.4	240.2	239.4	4930	1.529	1.208	1.393	117.7	74.6	11.1	5.91	2.38	15.5
		50-65	1011	588.6	1.692	0.811	2.087	235.1	240.8	240.0	4947	1.529	1.205	1.398	118.1	70.3	11.1	5.92	2.25	15.5
		70-80	1006	585.4	1.788	0.745	2.399	231.1	236.4	235.6	4868	1.527	1.210	1.407	112.9	62.3	10.5	5.68	2.01	14.8
		105-120	1007	582.7	2.031	0.682	2.977	214.8	219.1	218.5	4549	1.519	1.268	1.426	85.0	49.6	9.3	4.48	1.62	13.3
294	6-26-56	20-25	995	575.0	1.603	0.877	1.828	231.8	237.5	236.7	4891	1.525	1.217	1.364	113.5	71.8	11.6	5.75	2.25	15.8
		30-45	998	576.7	1.555	0.984	1.581	227.1	232.6	231.9	4789	1.526	1.225	1.369	105.4	71.0	12.0	5.37	2.23	16.4
		50-60	998	577.8	1.518	1.087	1.396	221.9	227.1	226.4	4669	1.529	1.239	1.374	96.2	67.9	13.1	4.96	2.[illegible]	[illegible]
		70-75	995	575.8	1.471	1.205	1.221	215.1	220.1	219.4	4530	1.528	1.269	1.378	85.0	66.1	13.8	4.48	2.09	18.9
		85-95	997	579.2	1.441	1.344	1.073	208.0	212.5	211.9	4363	1.534	1.296	1.384	76.2	62.0	12.1	4.11	1.97	16.7
295	6-27-56	30-45	995	578.5	1.490	1.173	1.270	217.3	222.7	221.9	4556	1.534	1.248	1.339	101.3	70.2	14.4	5.26	2.16	19.2
		50-65	999	583.7	1.463	1.302	1.124	211.2	216.1	215.5	4407	1.542	1.269	1.347	89.9	66.4	14.0	4.74	2.05	18.8
		75-85	1005	587.9	1.538	1.078	1.427	224.7	230.1	229.4	4685	1.543	1.255	1.344	103.2	71.8	12.5	5.39	2.21	16.8
		95-100	1005	586.5	1.587	0.950	1.670	231.2	236.8	236.0	4831	1.540	1.250	1.347	110.5	71.7	12.8	5.75	2.21	17.1
297	9-19-56	60-80	998	703.5	2.000	0.984	2.031	235.8	240.8	240.0	4999	1.518	1.113	1.492	139.8	74.3	2.9	6.46	2.54	4.3
298*	9-20-56	3-7	930	652.3	2.085	0.837	2.492	223.3	--	--	4733	1.518	.837	1.446	168.5	57.6	8.0	6.76	1.91	11.5
		25-40	978	687.0	1.959	0.952	2.058	236.1	--	--	4995	1.521	.952	1.470	151.2	71.4	9.5	6.77	2.40	13.9
		50-60	989	694.9	2.012	0.938	2.145	235.6	--	--	4981	1.522	.938	1.490	146.6	66.3	8.5	6.42	2.26	12.6
299**	10-1-56	40-60	1000	692.6	2.005	0.909	2.206	237.7	--	--	4977	1.537	909	2.005	150.0	96.0	--	6.51	1.87	--

*Nozzle regeneratively-cooled by the fuel (ammonia)

**Nozzle regeneratively-cooled by the fuel (ammonia) and combustion chamber and turbulence ring regeneratively-cooled by the oxidizer (RFNA)

APPENDIX F

EXPERIMENTAL ERRORS

Errors in the measured values of P_c, F, $\dot{m}_o$, $\dot{m}_f$, r, I_s, c^*, and C_F were computed for each run. The method employed for calculating the errors in those parameters is described in detail in Reference 3, Appendix B. Briefly, the errors computed were the maximum errors due to the combination of (1) the estimated error in each calibration standard, (2) the estimated errors in the values of the orifice coefficients and the propellant specific gravities, (3) twice the standard deviation of the calibration points of the force and pressure pickups (calibrated before, and usually after, each run) from the least-squares equation fitted to the calibration points, and (4) the estimated uncertainty in reading the chart records. Table 8 lists the largest error in each parameter computed for any of the runs and the average error in each parameter for all of the runs; estimated errors in q_n and q_c are also listed.

The orifice meters used for measuring the propellant flow rates and the coolant flow rates were calibrated with water both before and after the acid-ammonia investigation. The acid orifice and the coolant orifices were calibrated over the range of Reynolds Numbers that occurred during the rocket motor runs. The ammonia orifice could not be calibrated at as high a Reynolds Number as was encountered during the actual runs; instead, the ammonia orifice was calibrated over a wide range of lower Reynolds Numbers, and the curve of orifice coefficient as a function of Reynolds Number obtained from the calibration was extrapolated to cover the Reynolds Number range of the rocket motor runs. The values of the orifice coefficients measured before the investigation began were employed in reducing the performance and heat transfer data. The calibrations of the orifice meters

made after the investigation was completed were of lower precision than the original calibrations; the second calibrations were made only for the purpose of detecting any large changes in the values of the orifice coefficients. The second calibrations had a precision of about ± 1 per cent, and the values of the coefficients given by the second calibrations were within 1 per cent of the values of the coefficients given by the original calibrations.

TABLE 8

Estimated Errors in the Measured Values

of Performance and Heat Transfer

Parameter	Maximum per cent error (largest value for any run)	Maximum per cent error (average value for all of the runs)
P_c	1.5	1.0
F	1.5	0.9
$\dot{m}_o$	1.4	0.9
$\dot{m}_f$	2.3	1.7
r	3.3	2.5
I_s	2.9	2.0
c^*	3.2	2.4
C_F	3.1	2.1
q_n	5.0	---
q_c	5.0	---

APPENDIX G

REFERENCES

1. Robison, D. E., and Elliott, D. G., "Experimental and Theoretical Performance Characteristics of White Fuming Nitric Acid and Jet Propulsion Fuel Rocket Propellants at High Combustion Pressures," Report No. F-55-2, Purdue University, Rocket Laboratory, June 1955. (Confidential)

2. Robison, D. E., "Experimental Rocket Motor Performance with White Fuming Nitric Acid and JP-4 at 1000 psia Combustion Pressure," Report No. I-53-4, Purdue University, Rocket Laboratory, May 1953. (Confidential)

3. Robison, D. E., Elliott, D. G., and Tucker, R. T., "Experimental Rocket Motor Performance with WFNA and JP-4 at 1500 psia Combustion Pressure and a Summary of the Effect of Combustion Pressure on Performance and Heat Transfer," Report No. I-55-1, Purdue University, Rocket Laboratory, February 1955. (Confidential)

4. Bartz, Donald R., "Experimental Rocket-Motor Performance and Heat Transfer of the RFNA-Ammonia Propellant System at Chamber Pressures to 2000 psia," Progress Report No. 20-268, Jet Propulsion Laboratory, California Institute of Technology, Pasadena, California, April 8, 1955.

5. Brinkley, S. R. Jr., Smith, R. W. Jr., Haben, M. A., and Edwards, H. E., "Thermodynamics of the Combustion Products of Ammonia with Nitric Acid," Report No. PX3-107/11, U. S. Bureau of Mines, Explosives and Physical Sciences Division, May 1953.

6. "Combined Bimonthly Summary," No. 7, Jet Propulsion Laboratory, California Institute of Technology, Pasadena, California, September 1948. (Confidential)